

Refereed Proceedings

Heat Exchanger Fouling and Cleaning:

Fundamentals and Applications

Engineering Conferences International

Year 2003

Fouling Enhancement under Flow Boiling
at Elevated Steam Qualities

S. J. Klimas
AECL

K. Fruzzetti
Electric Power Research Institute

J. M. Pietralik
AECL

R. L. Tapping
AECL

FOULING ENHANCEMENT UNDER FLOW BOILING AT ELEVATED STEAM QUALITIES

S. J. Klimas¹, J. M. Pietralik¹, K. Fruzzetti² and R.L. Tapping¹

¹ Atomic Energy of Canada Limited, Chalk River, Ontario, Canada K0J 1J0, email addresses: KlimasS@aecl.ca, PietralikJ@aecl.ca, and TappingR@aecl.ca

² Electric Power Research Institute, 3412 Hillview Avenue, California, U.S.A. 94304, Kfruzzet@epri.com

ABSTRACT

Under laboratory conditions of flow boiling in water at 272–285°C (5.7 to 7.0 MPa), it has been observed that fouling rates by colloidal iron oxides ("crud") dramatically increase upon reaching a certain steam quality and mixture velocity. In loop tests, an increase in fouling rates by up to 3 orders of magnitude was repeatedly observed. This effect is called here "heavy fouling under elevated steam quality" (HFESQ).

HFESQ is potentially very significant for once-through steam generators, and very large versions of recirculating nuclear steam generators, because it can lead to heavy fouling in the upper tube bundle.

The mechanism of HFESQ is not certain, but its onset appears to be associated with significant droplet entrainment after the transition of flow to the annular pattern. The postulated connections between the flow pattern and the fouling mechanism will be discussed. This mechanism may also be the reason for an increased rate of flow-accelerated corrosion at high steam quality in piping and piping fittings.

Experimental data will be shown suggesting that the onset of HFESQ is susceptible to the chemistry and size of the crud particles. This offers a route for possible mitigation of the fouling problem.

INTRODUCTION

Steam generator (SG) fouling is an endemic and costly problem in pressurized water and pressurized heavy water reactor power plants (PWRs and PHWRs). The thermohydraulic conditions on the SG shell-side, where the fouling occurs, depend on the details of the SG design.

For CANDU-6[®] SGs, the typical thermohydraulic conditions in the tube bundle are: pressure 4.8 MPa (absolute), saturation temperature 261°C, steam quality ranging from 0 to 0.25, mass flux 100 to 500 kg/m²s, heat flux 100 to 300 kW/m², and velocity up to 7 m/s. The mass fluxes and flow velocity are significantly higher at the tube support plates. Primary steam separators have steam quality up to 0.8.

SGs of the most recent designs tend to be larger and operate at higher pressure than the older, smaller ones. They may also feature higher local steam qualities in the upper tube bundle. For example, one commercial SG may have a steam quality reaching 0.62 in the top of the tube bundle. Once-through SGs (OTSGs) cover the entire range of steam qualities up to pure steam.

As a rule, recirculating SGs operate using all-volatile water treatment (AVT), i.e., the feedwater contains a volatile organic amine, e.g., morpholine or ethanolamine, for pH control (usually pH_{25°C} between 9 and 10), and residual hydrazine (often between 50 and 100 µg/kg) for oxygen-free operation. The SG feedwater is very pure, e.g., CANDU specifications call for iron concentration <5 µg/kg in the SG feedwater. Some power plants achieve feedwater iron concentration as low as 1 µg/kg. Other impurities are also monitored and limited to similarly tight specifications. Still SG fouling, mostly by iron-based corrosion products ("crud") remains an expensive issue.

The deposits mostly form on heat-transfer surfaces, where they are undesirable because they can:

- create flow-restricted or liquid-deficient zones, where aggressive chemistry may develop, resulting in under-deposit or crevice corrosion,
- have detrimental effects on heat transfer, resulting in degradation of plant thermal performance,
- cause flow blockages, resulting in an increased pressure drop and, in extreme cases, SG level oscillation.

Generally, the effect of crud is more detrimental the more non-uniform its distribution inside the SG.

Atomic Energy of Canada Limited (AECL) and Electric Power Research Institute (EPRI) have been examining the role of water chemistry on the rate of SG fouling by iron corrosion products under a range of SG "typical" thermohydraulic conditions (Turner et al., 1997, 2001, Klimas et al. 2002). The focus was to optimize the chemistry to minimize SG fouling rates, thus promoting removal of the corrosion products from the SG with the blowdown. The effect of thermohydraulic conditions on fouling rates was a secondary aspect to the water chemistry effect in this applied investigation. This paper presents results on what appears to be a sharp discontinuity of the fouling rates at a certain threshold of steam quality under otherwise constant conditions.

EXPERIMENTAL METHOD

The fouling tests were performed in a high-temperature water-recirculating loop (AECL H3 Loop, Fig. 1). The loop was pressurized with a positive displacement pump, and the pressure was controlled by a pressure-control valve located downstream of the main loop cooler. The flow rate was adjusted by altering the length of the pump stroke. The flow

rate was measured on-line using a positive displacement flowmeter, which had been calibrated using an accurate water-collection method (estimated $\pm 1\%$ accuracy) under test condition. An interchanger preheated the water entering the test section using the steam-water mixture exiting the heated test section. The test section inlet temperature was maintained at $\pm 1^\circ\text{C}$ by utilizing an interchanger by-pass. The working fluid was condensed, cooled to room temperature, and returned to the main make-up tank.

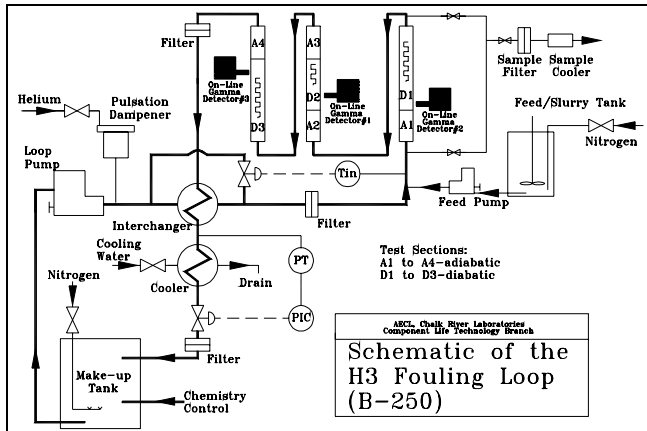


Fig. 1 Schematic of the Test Loop

The loop was fitted with a multi-segment, tubular test section, which was a pressure boundary. The test section employed direct electrical heating with alternating (60 Hz) current, i.e., the test section tubing itself was used as an electrical resistor. This method assured uniform heating, or a constant heat flux mode. Currents up to 1000 A were employed for heating. All heated sections were electrically isolated from the balance of the loop using ceramic insulators, and there was no interference between the heating and the loop instrumentation. The direction of the water/steam flow in the test section was vertically upward.

The magnetic flux density inside the test section was measured to be 2 mT or less (depending on the orientation) during a typical fouling test (Turner et al., 1999). A laboratory-settling test showed that a magnetic field of this order of magnitude was expected to exert a negligible force on a magnetite particle when compared to gravity.

The test section material (fouling substrate) was Alloy 600 (UNS N06600) or 800 (UNS N08800) commercial-grade tubing (ASTM B163 or B167) with inner diameter between 7.3 and 10.7 mm with the arithmetic average surface roughness height of $\sim 1.2 \mu\text{m}$. Alloy 600 contains Ni (min. 63%), Cr (14-17%) and Fe (6-10%) as the major components. Alloy 800 contains Ni (30-35%), Fe (39.5% min) and Cr (19-23%). New tubing was used for each test. The tubes were used "as manufactured" with the surface intact. The test section consisted of seven tubular

test pieces arranged in series (Fig. 1), four of which were unheated (adiabatic), the remaining three were heated (diabatic). The adiabatic pieces were located at steam qualities of about -0.25 , $+0.05$, $+0.25$, and $+0.50$. The total length of the heated sections was 4.1 m. The rate of heat addition to the heated sections was measured separately on each test piece, using a high-accuracy multi-channel voltmeter (Keithley 2000, 6.5 digits, $\pm 0.1\%$), and a high-accuracy current transformer ($\pm 0.1\%$) and an ammeter ($\pm 0.2\%$). The phase angle of the heating power was verified to be 0 (Yokogawa WT110, $\pm 0.25\%$). The total measurement error of the heat generation rate was estimated at $\pm 0.5\%$. All test section pieces were thermally insulated to prevent losses to the environment. Thus, the local heat flux and thermodynamic steam quality could be calculated for each axial position. The efficiency of the insulation was confirmed using a heat-flux meter, which showed a typical heat loss of 50 W per meter length of the test section (1.5 kW/m^2 based on the tube inner diameter). The thermal efficiency of the heated test section was determined from a heat balance under single-phase conditions conducted before each test. This efficiency typically exceeded 97%. Most of the heat losses occurred on fittings between the test section segments, and in the branching instrument lines and metal cables, resulting in a good estimate of local heat flux ($\pm 3.5\%$), but a relatively less accurate estimation of the local steam quality (± 0.015 , assuming thermodynamic equilibrium). The thermohydraulic conditions are listed in Table 1 and the water chemistry conditions in Table 2. The pH-controlling agents used in the loop tests are listed in Table 3 together with the concentration required to achieve the $\text{pH}_{272^\circ\text{C}} = 6.2$ at $X = 0$ specified for the tests.

Table 1. Loop Thermohydraulic Conditions

Parameter	Units	Standard Value	Alternative Values*
Pressure (Absolute)	MPa	5.7	6.5, 7.0
Saturation Temperature Water	$^\circ\text{C}$	272	280, 285
Temperature at Test Section Inlet	$^\circ\text{C}$	180	200
Mass Flux	$\text{kg/m}^2\text{s}$	300	660
Heat Flux	kW/m^2	230	410
Mass Steam Quality	Dimensionless	-0.3 to +0.55	

* Selected to envelop the range of conditions of interest.

Table 2. Loop Chemistry Conditions

Parameter	Units	Tests with Magnetite, Station Crud, and Ferrous Precipitates	Tests with Hematite, and Lepidocrocite
pH ₂₇₂ (at X = 0)	pH units	6.2	6.2
[O ₂]	µg/kg	< 5 (below the detection limit)	~150
[N ₂ H ₄]	µg/kg	25-100	0

Table 3. pH Controlling Agents and Their Nominal Concentrations

Name	Abbreviation	Concentration mg/kg	pH _{25°C}
Morpholine	MPH	10.7	9.26
Ethanolamine	ETA	4.3	9.53
Ammonia	NH ₃	2.6	9.64
Pyrrolidine	PYRR	0.97	9.13
3-Methoxypropylamine	3MPA	7.3	9.7
4-Aminobutanol	4AB	2.9	9.44
Potassium hydroxide	KOH	0.47	8.93
Dipropylamine	DPA	1.8	9.24
Dimethylamine	DMA	0.63	9.14
Dodecylamine	DDA	1.2*	9.58
Decylamine	DA	0.30*	9.54

* Used only in a mixture with 4.3 mg/kg of ETA

Several types of crud were used in the loop tests as the fouling species, all of them iron-based. The characteristics of these cruds are described in detail elsewhere (Turner et al. 1997, Klimas et al., 2002). Briefly, synthetic magnetite, Fe₃O₄, (particle diameter ~0.2 µm) was used as the fouling species in most of the tests. Two tests employed magnetite with a surface purposely contaminated with silica (a common station impurity). Two tests used a crud collected in a CANDU SG (85% magnetite and 15% hematite, particles 0.1-10 µm, volume average diameter 1.6 µm). Several tests used hematite, α-Fe₂O₃, which was either commercial grade (“Fisher Scientific”, 0.1 µm diameter) or manufactured at AECL (~0.2 µm diameter). Lepidocrocite, γ-FeOOH, was manufactured at AECL (rods, 0.2 µm length, aspect ratio ~10). Fresh ferrous precipitates were allowed to form in the loop during the test by a continuous injection of ferrous acetate at a rate very low compared with the loop flow rate. High-temperature filtration using 0.2 µm filters showed that over 99% of the iron was in particulate form. The cruds (or iron metal for preparation of radiotraced solutions) were irradiated in a nuclear reactor (“NRU” at AECL) to produce a radioisotope of iron (59-Fe, half-life 44.6 d). This radiotracer was employed for on-line monitoring of the rate of crud buildup at several locations on the heated test section using high-efficiency (high-purity Ge

monocrystal) γ-ray detectors. These “on-line data” were calibrated after the test by a precise determination of the distribution of the radioactivity along the test section.

Each loop test consisted of five consecutive phases: (1) the initial radioactive background count and test section conditioning at the experimental conditions (t < 0 h), (2) the fouling phase (0 h < t < 48 h), (3) the deposit removal phase (typically 48 h < t < 120 h), (4) loop shutdown, and (5) the final background count after the test section was removed (t > 120 h) (Fig. 2). The crud was injected into the loop during the fouling phase at a location approximately 2 m upstream of the inlet to the test section. The target concentration of crud in the loop water was between 0.2 and 0.6 mg/kg. Only a small fraction of the injected crud deposited on the test section during a typical test; the excess was removed from the flowing water on a system of filters downstream of the test section. During the course of the test, the loop water was periodically sampled at the inlet to the test section to determine the absolute radioactivity of the crud carried in water (A_{susp}, Bq/kg of water). At t ≈ 48 h, the dosage of radioactive crud to the loop was terminated, and the crud concentration promptly dropped by approximately one order of magnitude.

The fouling rates were calculated for each of the 29 pre-selected locations on the test section from the surface loading of the radioactivity, A_s, (Bq/m²), the radioactivity of the loop water, A_{susp} (Bq/kg), and the disintegration rate measured by the nearest on-line detectors, I_{on-line} (counts/s):

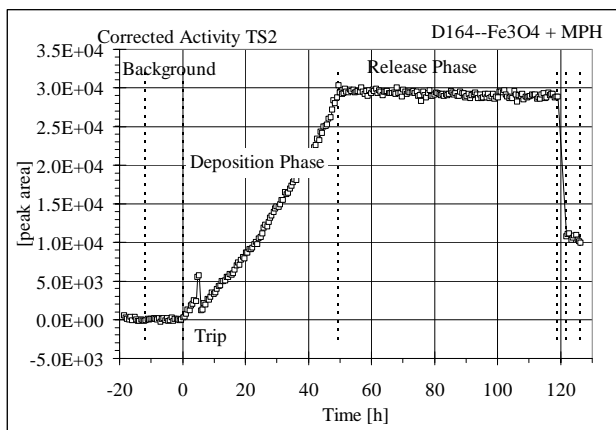
$$\frac{dm_d}{dt}(t, x) = \frac{1}{I_{on-line, final_count}} \frac{dI_{on-line}(t)}{dt} \cdot \frac{A_s(x)}{A_{susp}(t)} \quad (1)$$

Equation (1) normalizes the fouling rate to a unit particle mass fraction, i.e., kg of crud per kg of water-steam mixture. Therefore, it is referred to as the “normalized fouling rate”. Note that the normalized fouling rate can be determined using Equation (1) without the explicit knowledge of the concentration of crud in the loop water (mg/kg) or the crud specific activity.

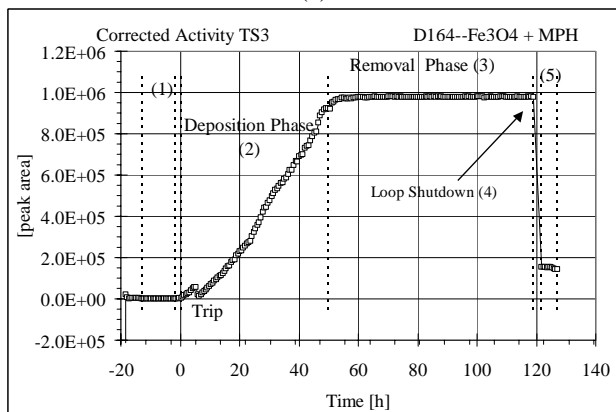
RESULTS

Fig. 2 reproduces two typical test curves showing the radioactivity measured by the on-line γ-detectors at two locations on the heated test section as a function of the time, low steam quality (X < 0.25) and elevated steam quality (X ≈ 0.5). The slope of the line during the fouling phase of the test is a measure of the fouling rate. For most tests, the fouling rates showed no obvious dependence on time; therefore, they were averaged for the duration of the fouling phase. However, some tests did exhibit variations of the fouling rates with time, up to a factor of 6, caused perhaps by (1) uncorrected variations in the crud concentration, (2)

changing conditions for bubble nucleation caused by fouling, and (3) different fouling rates on bare surface versus surface covered with deposits. During the removal phase, the example curves remain almost flat, indicating that no significant removal of the deposit from the surface was taking place during this phase. The dependence of the removal rates on water chemistry have been analyzed elsewhere (Turner and Klimas 2001, Klimas et al. 2002). Linear steady-state fouling is predicted by the AECL fouling model which represents fouling as a sum for three fundamental processes: particle deposition (transport and attachment to the wall), deposit consolidation, and re-entrainment of unconsolidated deposits.



(a)



(b)

Fig. 2 Typical Test Curves with MPH Chemistry for (a) Region of Low Steam Quality and (b) Region of Elevated Steam Quality

An example of the normalized fouling rate as a function of steam quality is shown in Fig. 3. The fouling rates are shown for both heated (circle markers) and unheated surfaces (square markers). The fouling rates increase in the region of subcooled nucleate boiling ($-0.25 < X < 0$) but remain relatively unchanged in the region of saturated nucleate

boiling ($0 < X < 0.25$). At steam qualities of between 0.45 and 0.53, the fouling rate increases by approximately 2 orders of magnitude. This sudden and significant increase in the fouling rate was termed “high fouling under elevated steam quality”, HFESQ. In the current work, we concentrate on fouling under flow boiling conditions. The data for forced convection (square markers on Fig. 3) were analyzed elsewhere (Klimas and Pietralik, 2002).

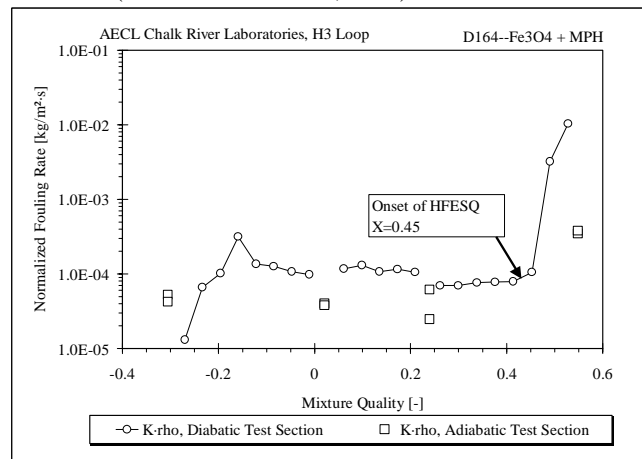


Fig. 3 Example of Experimentally-Determined Dependence of Fouling Rates on Steam Quality on Heated and Unheated Surfaces

Fig. 4 shows the results of an examination of the test section after the test. Fig. 4a shows a photograph of a sample of the test section that was cut open. This sample was selected from the test section region undergoing HFESQ as per Fig. 3. The steam qualities in this fragment ranged from 0.49 (inlet to the shown fragment, bottom) to 0.52 (outlet, top). The outlet region has a visibly higher deposit loading (darker color) than in the inlet (lighter shade). Scanning electron microscopy (SEM) micrographs of two coupons from the same fragment are shown in Figures 4b and 4c. The surface from the inlet (4c) is mostly bare metal, with numerous deposit particles scattered in the field of view. The surface at the outlet (4b) is completely covered with crud. From the measured surface radioactivity, the surface loadings on these coupons were 0.038 and 3.8 kg/m², respectively (assuming magnetite as the only fouling species), which corresponds to 2.6% and 259%, of a monolayer of particles, assuming closed-packed spheres of the original crud particles. These coverages are consistent with the deposit appearance on the micrographs. Many of the deposits (including the sample shown in Fig. 4b) appear crystalline, and this has been tentatively attributed to the re-crystallization of the original crud particles. This explanation is favored because the degree of crystallinity appears to increase with the increasing duration of the test. However, a role of dissolved species in the formation of crystals as in Fig. 4b cannot be excluded.

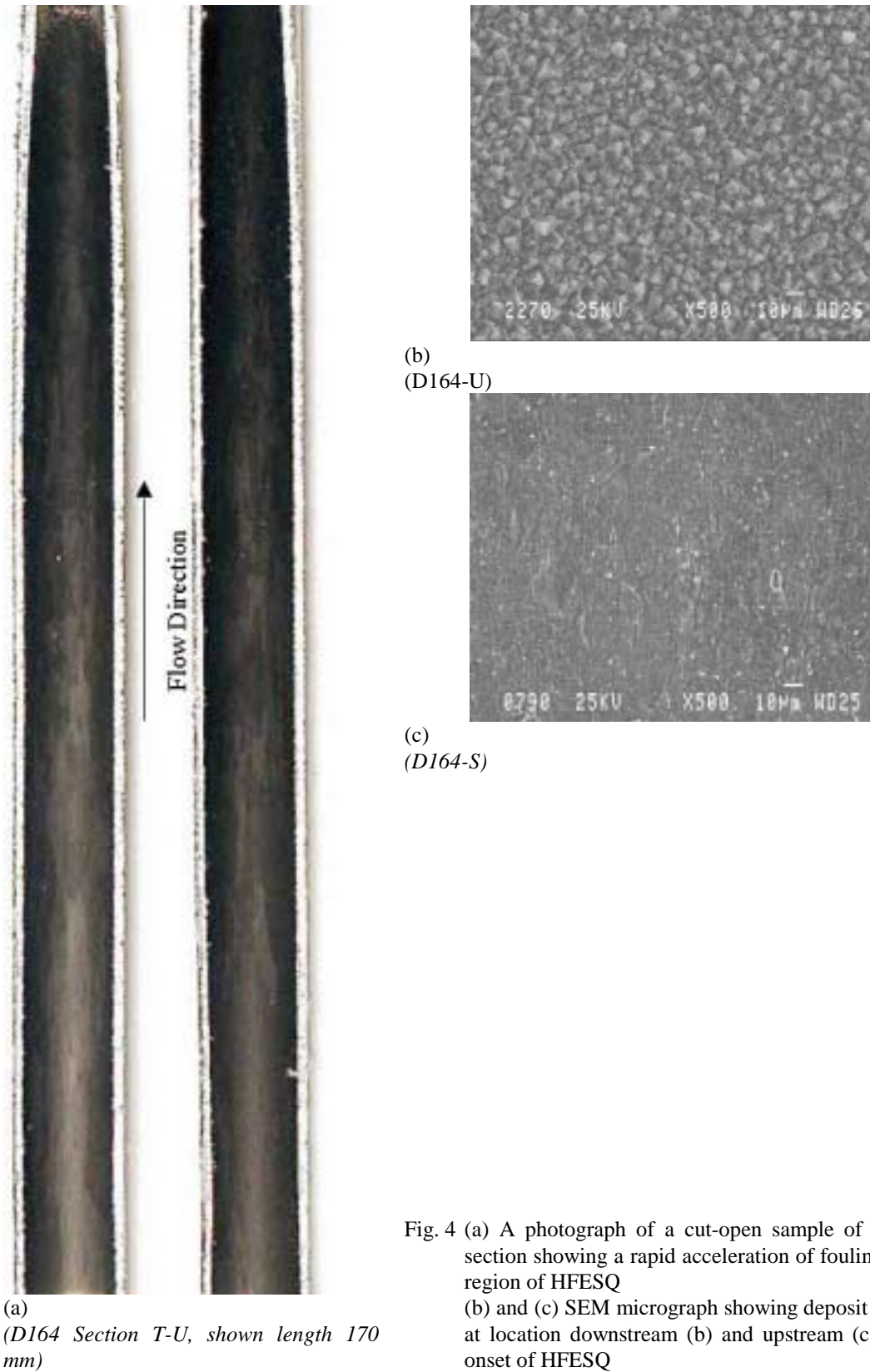


Fig. 4 (a) A photograph of a cut-open sample of the test section showing a rapid acceleration of fouling in the region of HFESQ (b) and (c) SEM micrograph showing deposit loading at location downstream (b) and upstream (c) of the onset of HFESQ

Fig. 5 summarizes results of 36 loop tests conducted with magnetite particles as the fouling species under constant thermohydraulic conditions. Each data point is an average of at least 2 test results. Constant high-temperature pH was used, but the pH was adjusted using 11 separate pH controlling agents, as labeled on the abscissa. The mean fouling rates at elevated steam quality ($X = 0.5$, circle markers) are compared to those at low steam quality ($0 < X < 0.25$, triangle markers) determined in the same sets of tests. In all instances, the fouling rates at elevated steam quality are higher than or equal to those at low steam quality (at constant chemistry). The increase of fouling rate at elevated steam quality was measured to be up to 3 orders of magnitude in some individual tests, yet was not observed at all in some others. The mean rate at elevated steam quality was 6.7 times larger than that at low steam quality. The water chemistries that appeared to produce relatively low or no HFESQ are the mixture of DDA with ETA, and 4AB, but this conclusion is tentative because of the small number of tests conducted under these two chemistries (2 tests for each).

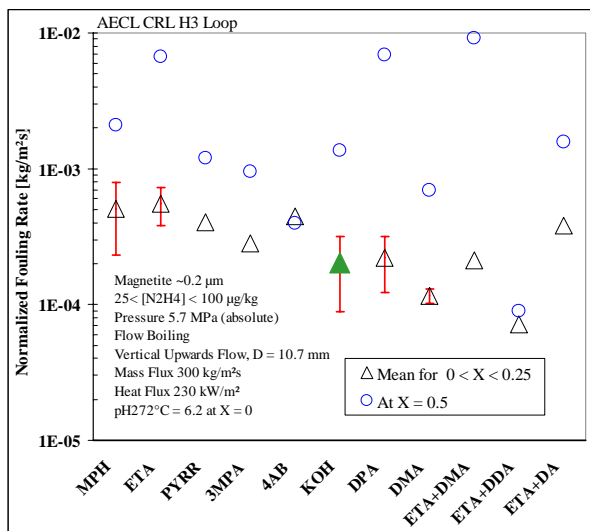


Fig. 5 Effect of Amine on the Magnitude of HFESQ for Magnetite Particles

Fig. 6 summarizes results of 19 loop fouling tests in which hematite particles ($0.1 \mu\text{m}$ diameter) were used as the fouling species. The pH was adjusted using the agents as labeled on the abscissa. For most tests, no HFESQ was observed. The exception was one test with DMA where HFESQ did appear. For tests with ETA the average fouling rates under elevated steam quality were actually diminished in comparison with those at $0 < X < 0.25$.

Fig. 7 summarizes results of 36 loop fouling tests conducted under water chemistry controlled with a single amine (MPH) but with different cruds. HFESQ occurred in most the tests with synthetic magnetite particles, as

described above. HFESQ was not well-pronounced in the tests with polydispersed "station" crud. HFESQ was not observed in any of the 5 tests with "fresh ferrous precipitates". This suggests that HFESQ occurs by a mechanism specific to particles. The data for hematite is ambiguous. Clear HFESQ was measured in 2 tests conducted with $0.2\text{-}\mu\text{m}$ hematite particles. No comparable data are available for the commercial hematite with smaller $0.1\text{-}\mu\text{m}$ particles, but HFESQ was not observed for several other hematite-amine combinations.

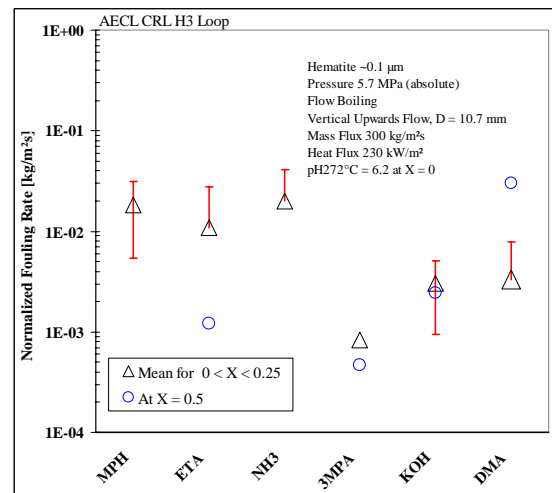


Fig. 6 Effect of Amine on the Magnitude of HFESQ for Hematite Particles ($0.1 \mu\text{m}$)

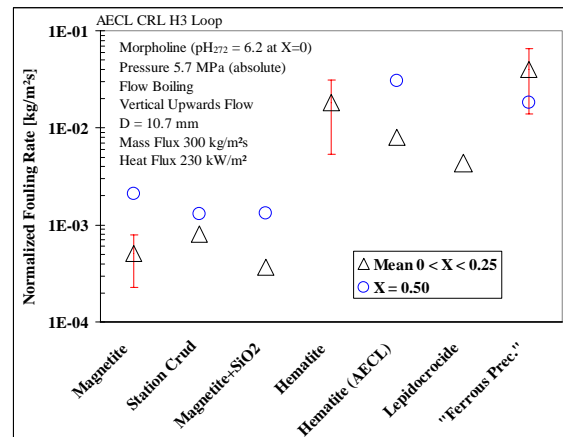


Fig. 7 Effect of Crud Type on the Magnitude of HFESQ for MPH Water Chemistry

Several additional loop tests were conducted with magnetite and MPH under "alternative" values of the thermohydraulic conditions (Table 4). The confidence interval for the average point of onset of HFESQ was quantified and is given in Table 4. HFESQ was never experimentally observed for $X < 0.35$.

Table 4. Mean Point of Onset of HFESQ for Magnetite Particles (pH controlled with MPH)

Thermohydraulic Conditions	X of onset of HFESQ, -	
	Mean	90% Confidence Interval
Standard	0.39	0.09
Alternative Mass Flux and Heat Flux	0.58	0.08
Alternative Pressure	0.50	0.03

DISCUSSION

The fouling rates under elevated steam quality show significant test-to-test variability. Part of this variability can be attributed to the design of the tests which were not optimized for measuring HFESQ; the test section terminated soon after the onset of HFESQ, and the fouling rates were quantified in a region of their steep increase (Fig. 3). However, it appears that the fouling rates at HFESQ is sensitive to water chemistry. This offers a possible route to mitigate the fouling problem.

The measured variability in the steam quality of onset of HFESQ significantly exceeded the measurement uncertainty. An explanation for this may require data covering a wider range of hydraulic conditions, and perhaps knowledge of the exact dependence of the flow pattern on the flow history and other minor test parameters.

The literature does not appear to record HFESQ as a significant phenomenon. LeClair (1966) reported doubling of the fouling rate at a steam quality estimated at 0.36. The conditions LeClair used were: pressure 6.9 MPa, mass flux 1060 kg/m²s, heat flux 735 kW/m², and neutral water. Thomas (1974) presented experimental fouling curves that indicate a small (up to 20%) increase in fouling at $X \approx 0.35$ at 21 MPa, mass flux 790 kg/m²s, heat flux 325 kW/m², with crud particles 20-50 μm in neutral water. However, SG inspection data do indicate enhanced fouling in some steam generators at regions of elevated steam quality (Staeble et al. 1996, Turner et al. 1999).

The understanding of HFESQ is not complete. It is believed that HFESQ occurs because of the flow pattern in the region of elevated steam quality, namely the “annular flow with significant droplet entrainment” (Fig. 8). The annular two-phase flow pattern occurs for significant fractions of gas phase and; under the test conditions, it starts at steam quality of about 0.2. At a high steam quality it changes to mist flow, where the liquid phase exists as small droplets. In the annular flow pattern, the wall is covered with a film of moving liquid. Vapour travels in the tube center region carrying droplets of liquid. The liquid film also contains bubbles created by boiling. It is quite common to find that a half or more of the liquid is flowing as droplets.

This flow pattern is dynamic in the transverse direction; the droplets are continually created by the interacting flowing phases and deposited on the liquid film. The mechanisms causing the formation of droplets are disturbance waves and bubble bursts at the liquid film surface. Disturbance waves are large waves occurring in the liquid film that can be ‘undercut’ by the flowing gas, thus forming small droplets that are carried by the gas phase. The bursting of steam bubbles by the flowing gas phase also creates small droplets. The droplet size is typically in a range of a fraction of a millimeter. At the same time, turbulence and large-scale motions of the core flow cause an intense motion of the gas core, including the droplets, in the direction perpendicular to the main flow direction. It was observed experimentally that, as a result of this intense motion, the concentration of droplets in the gas region is practically uniform. Consequently, the droplets also hit the surface of the liquid film and deposit on it. The two processes are called film entrainment and droplet deposition. Under a given set of thermohydraulic conditions, an approximate steady-state is established between the two processes: the rate of both is the same. Because the droplets carry crud particles, on droplet impact onto the wall the crud particles are transported to the wall where they can deposit. Because the rate of entrainment (and deposition) is high, there is a high mass transfer coefficient carrying the crud from the core to the liquid film and further to the wall.

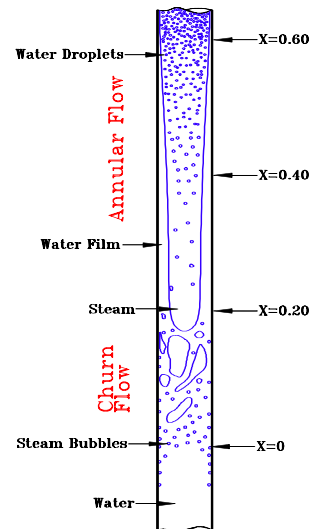


Fig. 8 Schematic of Flow Patterns for Two-Phase Flow in Heated Tube (Turner et al., 1999).

The deposition and re-entrainment of liquid droplets has been described by empirical correlations, including the Govan correlation (Hewitt and Govan, 1990; Barbosa et al., 2002; Pan and Hanratty, 2002). Droplet deposition fluxes as high as 0.5 kg/m²s are predicted by applying the Govan correlation to our test setup. This number represents the

upper limit for fouling by the proposed mechanism under the investigated test conditions, i.e., this would be the normalized fouling rate if all the particles carried in the deposited droplets attached to the tube wall. The loop experimental data suggest that this limit may be approached under some chemistry conditions, implying no effective removal under the experimental conditions.

The hydraulic phenomenon that causes HFESQ may have implications in other fields where mass transfer plays a role, e.g., flow-accelerated corrosion (FAC).

CONCLUSIONS

The major conclusions from this work are as follows:

1. Under conditions relevant to recirculating steam generators (SG), very high fouling rates by iron corrosion products are possible at elevated steam qualities ($X \geq 0.35$). This phenomenon is called here "high fouling under elevated steam quality", HFESQ. Increases in fouling rate by up to 3 orders of magnitude were measured in the loop tests under simulated SG operating conditions.
2. HFESQ appears associated with a specific two-phase flow pattern (annular flow) and appears to occur only when crud particles of a certain minimal size are present.
3. The magnitude of HFESQ appears sensitive to water chemistry. This offers a route for possible mitigation of this fouling problem.
4. The hydraulic phenomenon that causes HFESQ may have implications in other fields where mass transfer plays a role, e.g., flow-accelerated corrosion (FAC).

NOMENCLATURE

A_s	surface loading of radioactivity, Bq/m ²
A_{susp}	radioactivity of the crud carried in water, Bq/kg
I	measured γ -ray activity (background-corrected), counts/s
m	surface loading, kg/m ²
T	temperature, °C or K
t	time, s
X	thermodynamic steam quality, mass-based, dimensionless
x	distance, m

Acronyms

AVT	all-volatile water treatment
CANDU®	CANadian Deuterium Uranium, a registered trademark of Atomic Energy of Canada Limited.
FAC	flow-accelerated corrosion
HFESQ	high fouling under elevated steam quality
PHWR	pressurized heavy-water reactor
PWR	pressurized water reactor
SG	steam generator (boiler)

Greek

ρ mass density, kg/m³

Subscript

d deposit

REFERENCES

- Barbosa, J.R., Hewitt, G.F., Konig, G., and Richardson, S.M., *Liquid Entrainment, Droplet Concentration and Pressure Gradient at the Onset of Annular Flow in a Vertical Pipe*, Int. J. Multiphase Flow, v. 28, pp. 943-961, 2002.
- Hewitt, G.F. and Govan, A.H., *Phenomenological modeling of non-equilibrium flow with phase change*, Int. J. Heat Mass Transfer, 33, No.2, 229-242, 1990.
- Klimas, S.J., Guzonas, D.A., Turner, C.W., and Fruzzetti, K., *Identification and Testing of Amines for Steam Generator Chemistry and Deposit Control*, Report 1002773, Electric Power Research Institute, Palo Alto, CA, U.S.A., December, 2002.
- Klimas, S.J. and Pietralik, J.M., *Two-Phase Forced-Convective Fouling Under Steam Generator Operating Conditions*, 4th Canadian Nuclear Society Steam Generator Conference, May 5-8, Toronto, Canada, 2002.
- LeClair, B.P., *Deposition on Boiling Heat Transfer Surfaces*, Report CEI-174, Atomic Energy of Canada Limited, Chalk River, Ontario, 1966.
- Pan, L. and Hanratty, T.J., *Correlation of entrainment for annular flow in vertical pipes*, Int. J. of Multiphase Flow, v. 28, pp. 363-384, 2002.
- Staehle, R.W., Diercks, D.R., Hall, J.F., Bryant, P.E.C., Keefer, R.H., and Woodman, B., *Local Chemistry and Deposit Formation at Upper Tube Bundle Free Span Region*, IRN16825949, pp. 79-83, NACE International, 1996.
- Thomas, D., "Experimentelle Untersuchung über die Ablagerung von suspendiertem Magnetit bei Rohrströmungen in Dampferzeugern" Brennst.-Wärme-Kraft, 26, Nr. 3, März, 1974.
- Turner, C.W. and Klimas, S.J. *The Effect of Surface Chemistry on :Particulate Fouling Under Blow-Boiling Conditions*, Heat Exchanger Fouling: Fundamental Approaches and Technical Solutions, Davos, Switzerland, July 8-13, 2001.
- Turner, C.W., Guzonas, D.A., Klimas, S.J., and Frattini, P., *Surface Chemistry Intervention to Control Boiler Tube Fouling*, Report TR-110083, Electric Power Research Institute, Palo Alto, CA, U.S.A., December, 1999.
- Turner, C.W., Klimas, S.J., and Frattini, P.L., *The Effect of Alternative Amines on the Rate of Boiler Tube Fouling*, Report TR-108004, Electric Power Research Institute, Palo Alto, CA, U.S.A., September, 1997.